INSTRUMENTAL EFFECTS IN SECONDARY ELECTRON YIELD AND ENERGY DISTRIBUTION MEASUREMENTS*#

Robert E. Kirby,† Stanford Linear Accelerator Center, Stanford, CA 94309, USA

Abstract

Measurement of secondary electron yields and electron energy distributions appears straightforward – simple equipment, simple electronics, easy-to-acquire data, at least in a laboratory setting. Unfortunately, the low secondary electron energy (2-5 eV) and the extreme sensitivity of the yield to surface condition and surrounding environment make the measurement details anything but simple. These problems affect the accuracy and interpretation of the experimental results, often in a subtle way. Most troublesome is the production of unwanted (and unexpected) secondary electrons from within the electron sources and detectors, and tertiary electrons from the surrounding vacuum chamber environment. In addition, the sample surface condition can change during measurement, for example, through electron damage or enhanced oxidation/carburization. Electron source, analyzer, and sample effects will be discussed.

INTRODUCTION

The general features of secondary electron emission are well understood [1]. Primary electrons impact the surface and either reflect elastically or suffer energy loss through a variety of channels: phonon and plasmon-generating loss, ionization of atoms, free-electron scattering, surface state capture, interband transition, etc. The electrons generated by these inelastic processes are referred to as "true secondary" while re-emitted primary electrons that suffer loss are classed as "re-diffused" primaries. Most secondaries are of very low energy (2-5 eV), a result of multiple collisions, and must be within a free path of the surface (1-3 nm in metals, ~100 nm in dielectrics) in order to escape into vacuum. It is this long free path in insulators, where the loss mechanism is mostly through defect scattering, that is responsible for their high secondary yield. In technical materials, however, defect scattering and surface layers have a major effect on SEY reduction. Such surfaces might be characterized as an agglomeration of semiconducting oxides and carbides, "glued" down with unpolymerized hydrorcarbons and water.

In the course of measuring secondary electron yields from various materials [2-5], using several methods, we have noticed and studied some data variations caused by 1) secondary "primary" electrons generated inside the electron source, 2) tertiary electrons generated from chamber walls and components, 3) tertiary electrons generated from the structure of the energy distribution measuring spectrometer, 4) sample surface modification by primary electrons and, 5) substrate backscatter contribution to the yield of thin overlayers. The presence of these effects is generally recognizable and preventable.

MEASUREMENTS

Yields are generally measured either by monitoring the sample current or by collecting the scattered primary and secondary emission with a retarding field analyzer (RFA) or biased Faraday cup. Each technique has defects which can contribute to potential misinterpretations of the data.

The simplest sample current method, the retarding potential (RP), consists in fixing the primary electron gun potential and then determining the final electron energy at the sample by voltage bias retardation. Fig. 1 shows the layout of this technique where the yield δ is determined from the sample and primary currents as

$$\delta = 1 - I_T/I_P$$

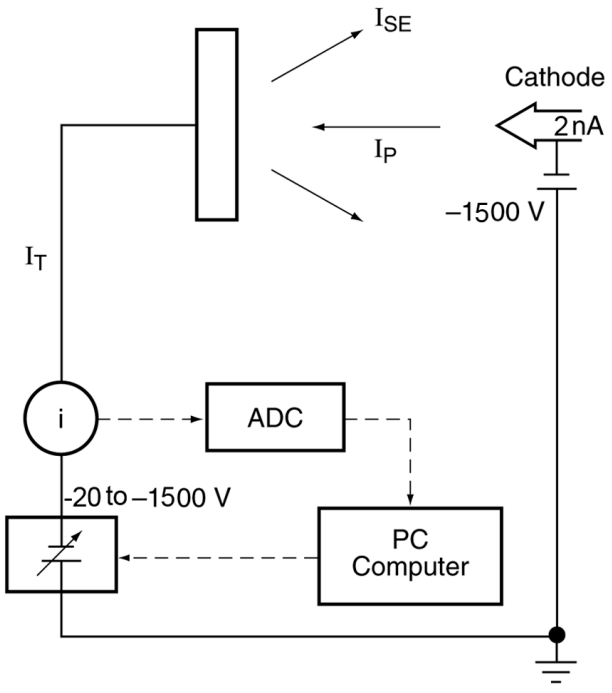

Figure 1: Retarding potential (RP) measurement layout. ADC= analog-to-digital converter. The "target" or sample current, I_T, is measured with a high voltage-isolated picoammeter.

To minimize modification of the sample surface by the primary beam, the primary current must be on the order of a nanoamp, with data collection of several minutes per

* Work supported by the U.S. Department of Energy under contract number DE-AC03-76SF00515 (SLAC).
# Detailed manuscript submitted to Phys. Rev. ST AB.
† REK@slac.stanford.edu

curve. That implies a desired sample leakage of 1 pA or less. Retard voltage scanning begins with a small bias on the sample of –20 V in order to prevent tertiary electrons from the chamber returning to the sample (this point will be discussed in detail later). Advantages of this technique are simple equipment and no space charge limit in the electron gun to achieve low (<200 eV) incident energy and, of course, stable primary beam current.

The RP technique cannot be used to measure the elastic backscatter coefficient nor the energy distribution curve (EDC) of the secondary electron spectrum. Commercial gridded (e.g., retarding potential) or differential (e.g., cylindrical mirror) analyzers used for these purposes usually collect only a portion of the 2π- steradian emission. In addition, the emission spectrum itself is not angularly uniform, even for polycrystalline samples, because the elastic backscatter is peaked sharply about the normal while the true secondaries are emitted in a cosine distribution. Therefore, a differential measurement is sure to get the relative population of each type wrong, at all angles.

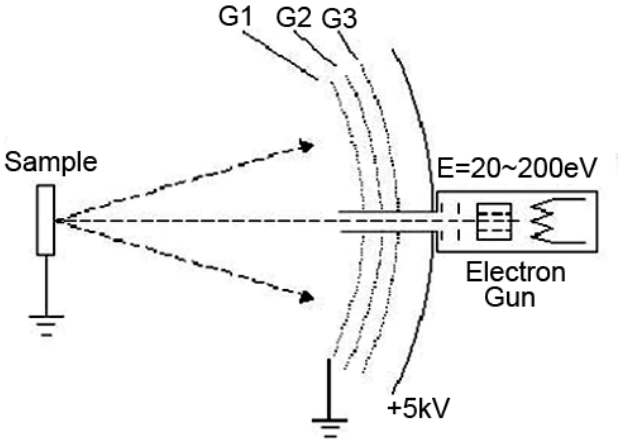

Figure 2: Retarding field analyzer schematic, showing the penetration of the gun drift tube through the grids and collector. G2 is the retarding grid for EDC measurements. G1 establishes a field-free region; G3 is an electrostatic shield grid.

A typical 120° acceptance angle RFA is shown in Fig. 2. A serious defect in this type of analyzer is the creation of tertiary electrons on the gun collimator, grid housing and grids. Some of these return to the sample while others, under some grid biases, can penetrate and reach the collector. There is no ideal solution to these problems and a combination of techniques and well-characterized instrumentation is essential to obtaining artifact-free data, especially at low primary and secondary energies.

RESULTS AND DISCUSSION

Electron source artifacts

From our earliest SEY measurements, we noticed that tuning of the electron gun focus lens could, in some instances, affect the shape of the SEY curve. An example of this effect is shown in Fig. 3 (sample current vs. retard voltage, for clarity) for sputter-cleaned Nb. The location of the unexpected "dip" in the data (solid circles), at approximately 750 V retard voltage, shifted correspondingly with electron gun focus lens setting.

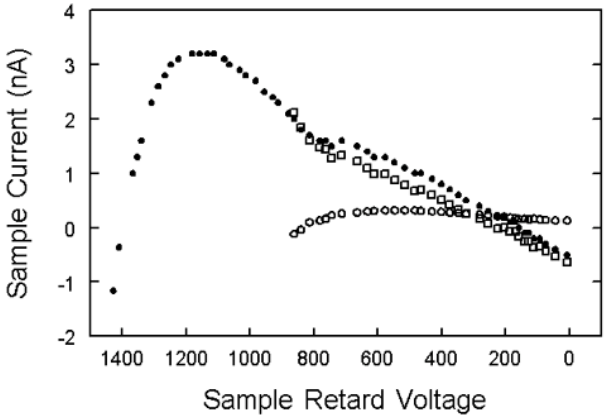

Figure 3: RP SEY from sputter-cleaned Nb, displayed as sample current. Shown is the sample current difference (open squares) after subtraction of scaled and shifted focus lens "primary" secondary current (open circles) from the original data (dots).l Cathode potential = –1500 V.

A measurement of the primary electron gun beam, with a Faraday cup (Fig. 4), found a halo of electrons present. Our energy analyzer confirmed the presence of a small elastically-scattered peak at 950 eV, in addition to the main component at 1500 eV. This current slice across the diameter gave a peak Faraday cup current of 0.6%. Integration of the entire halo current yields ≈12.5% of the main beam. We scaled the original data (solid circles) of Fig 3 by 0.1 and shifted it by +550 V (the focus lens potential relative to the cathode potential) to give the approximate contribution of the focus lens "primary" secondary electrons, Fig. 3 (open circles). When this

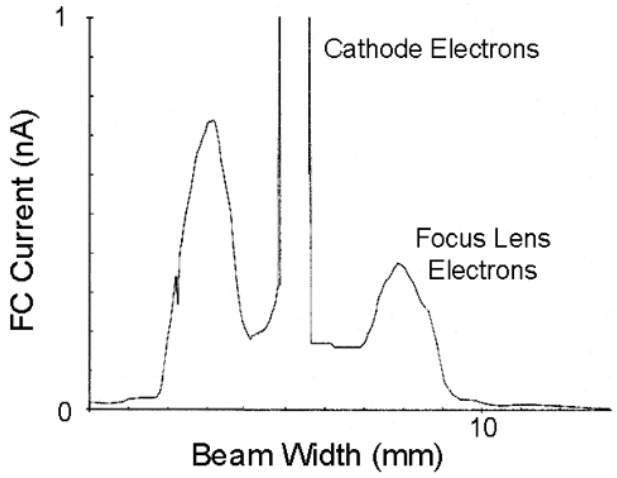

Figure 4: Faraday cup (0.25 mm diameter circular aperture) measurement of current leaving the electron gun used to collect Fig. 3. The asymmetric "halo" is due to secondary electrons generated from the focus electrode by cathode electrons.

contribution is subtracted from the sample data, the dip is reduced and the current slope is corrected Fig. 3 (open squares).

Finding which gun element was responsible, in this case, was easy because of the simplicity of the gun element structure (Fig. 5). The focus lens was the only element not at cathode or ground potential. This type of gun derives its voltages from a single high-voltage source and a resistive divider ("unipotential"). This is the classic gun structure of the monochrome television, whose principle defect for use as a primary electron source is severe space charge at low cathode potentials (< 200eV).

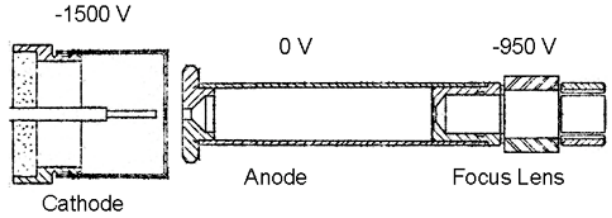

Figure 5: Commercial [6] unipotential electron gun used to collect data of Fig. 3 in RP mode. The downstream element of the focus lens ("–950V") is the source of the secondary electrons that strike the sample. Voltage labels are relative to ground.

More sophisticated gun structures have been designed and manufactured that overcome the cathode space charge limitation directly by using a combination of fixed high voltage cathode potential followed by a retarding "zoom" lens that decelerates the beam to final energy near the gun downstream end. The beam then drifts to the sample. Such guns are capable of operating down to less than 10 eV. Primary electron energy is changed by varying the cathode potential (VC).

As in the unipotential gun, improper setting of gun potentials leads to secondaries being generated on elements (probably at aperture edges).Some of these escape the gun and form one or more primary "secondary" sources. An example of this is shown in Fig. 6 for incorrectly set anode and focus lens potentials.

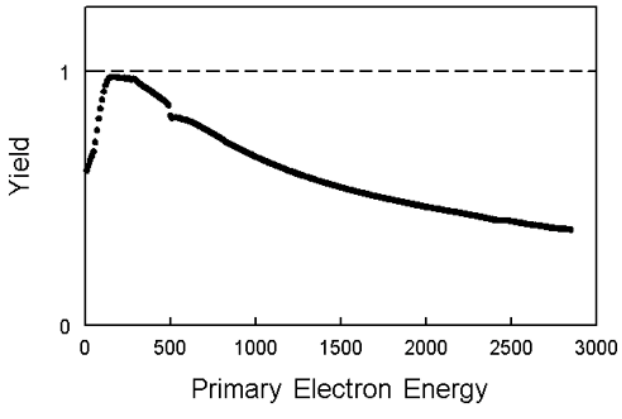

Figure 6: VC SEY data from graphite [7], sputtered-cleaned, with anode potential mistuned to cause secondary electron generation from the anode aperture A of the gun.

Tertiary electron production

All but the lowest energy secondary and elastically-reflected electrons leaving the sample and striking nearby components and the chamber wall are capable of generating tertiary electrons, some of which may return to the sample. The easiest way to prevent these tertiaries from hitting the sample is to apply a small negative bias to the sample. The effect of tertiaries and bias is shown in Fig. 7. Tertiaries reduce the total current leaving the sample surface because of their low energy ($\delta<1$).

In the Experimental Details section, mention was made of this tertiary-rejecting bias (shown in Fig. 1). SEY data taken by both methods, RP and VC, are plotted in Figure 8. In the RP case, the first -20 V of retard data is discarded; in the VC case, the bias is a constant –20 V. The agreement is generally good. The disagreement at lowest energy on this specific sample is possibly due to conditioning of the delicate native oxide in the RP measurement, because the lowest energy primaries are deflected over to an unconditioned portion of the sample, giving a slightly higher yield.

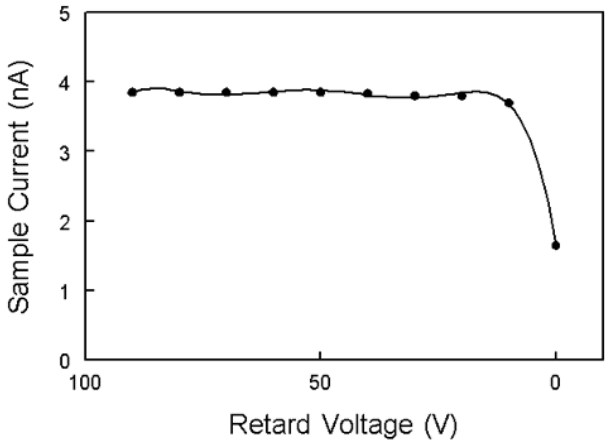

Figure 7: RP data from sputter-cleaned Al covered with native oxide. At –10 V retard most of the tertiary electrons from the surrounding chamber are rejected.

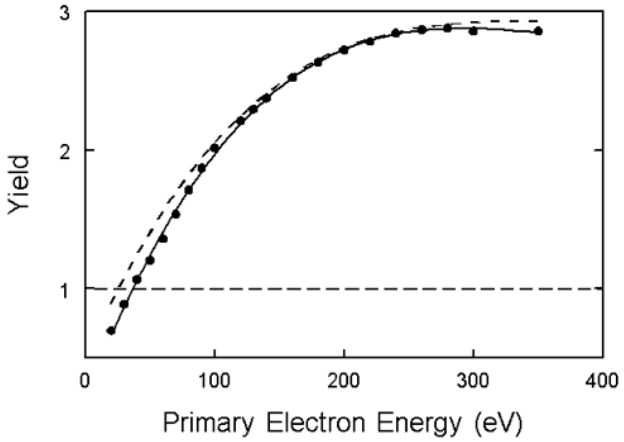

Figure 8: SEYs from sputter-cleaned Al with a native oxide. Displayed are an RP (solid line) and VC (dashed) SEY of the same surface area.

Measuring the SEY with an RFA does not avoid the tertiary problem. Elastic and secondary electrons from the sample strike the RFA and generate tertiaries on the grid housing, gun collimator and grids. Depending on grid biasing some of these will make it to the RFA collector while some return to the sample. Figure 9 is RFA data from Cross [8] showing the creation of teriaries on the inner grid and on the collimator. In the RFA, tertiaries are generated at the gun collimator (V=0), at the field-free inner grid (closest to the sample, also usually V=0) and on the negative retarding grid (when collecting an EDC). For the figure data, the retarding grids were biased a few volts positive to increase collection of the tertiaries and separate the collimator tertiary electrons from the inner grid tertiaries. Tertiaries make their way to the collector through grid penetration at high (typically, several kV) RFA collector biases, or through direct generation on the negative retarding grid. Electrons generated from the sample can be distinguished (except for elastics) from those generated elsewhere in the system by applying a small negative bias to the sample. Sample secondaries will shift to higher energy in the EDC spectrum, by the sample bias amount. Characterizing the behavior of the RFA , particularly at low energy, is essential to sensible interpretation of results at low energy. Many discussions of these problems can be found in 1970s publications describing low energy electron diffraction equipment.

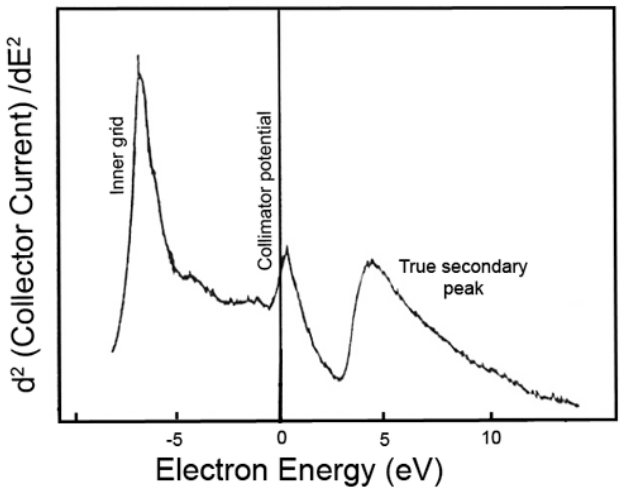

Figure 9: Tertiary electron spectrum generated inside a retarding field analyzer from its gun collimator and the grid closest to the sample [8]. The sample has been biased –3 V to separate the sample secondaries from the RFA tertiaries.

Surface modification by incident electrons

These changes are loosely grouped as "electron conditioning" and include desorption, carburization, oxidation, and damage. Desorption of surface gases and the carburization of carbon-containing molecules on the surface have a dramatic effect on SEY. Studies have shown that H, CO, CO2 and CH4 are electron-desorbed from Al extrusion, with H and CO2 having an initial rate of 1 molecule/electron [9]. The chemical state of the carbon influences the SEY through the emission transmission probability. The probability is increased by up to 50% for water and aromatic hydrocarbons and reduced by up to 50% for polymerized and elemental carbon [10]. The mechanism is the hybridization of molecular surface states with conduction band electrons. The transmission of secondaries is controlled through the elastic/inelastic crossection at the surface barrier.

Oxidation of surface metal atoms is encouraged by the ability of the electron beam to dissociate water and create OH– [11]. Perfect oxides have high yields but defective oxides, such as are produced by electron impact, can reduce the SEY. These sub-oxides are semiconductors that contribute both electron-electron and defect-electron scattering, thus reducing the SEY. TiO_2 is the prototype metal oxide surface, whose defect structure has been studied extensively [12,13].

Finally, an unusual source of surface CO was found at SLAC in 1968 [14]. Under electron bombardment, bulk CO was observed to move up the grain boundaries to the surface of Al covered by a thin layer of γ-Al_2O_3. This was confirmed by the use of CO^{18} adsorption from the gas phase. Thus, in some cases, the bulk can be an important source of carbon for SEY reduction during the conditioning process.

Substrate backscatter effect

SEY enhancement via primary electron backscatter is not normally a problem unless the SEY-suppressing overcoating is very thin, <1.5 nm in the case of TiN-coated klystron windows, for example. Monte Carlo simulation of the penetration of 500 eV primary electrons into TiN, at normal incidence, shows that the range is 2-3 nm. This means that backscattered primaries from the substrate will penetrate the overlayer on return to the surface, thereby enhancing the SEY. Fig. 10 illustrates this effect for TiN overlayers on Nb. The difference in yields, based on TiN thickness, increases from 50 eV up to 750 eV or so where the primary electron range is large compared to overlayer thickness (50 nm at 3 keV). This effect is important in cases, such as the coating of klystron windows where the overlayer thickness must be effective for SEY reduction but not so thick as to cause ohmic heating in operation.

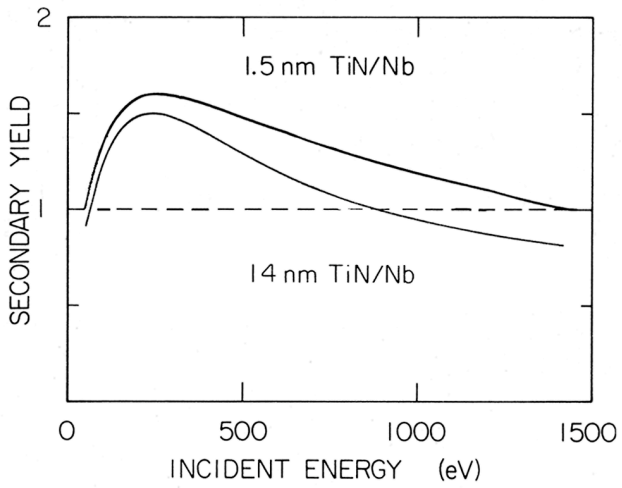

Figure 10: RP SEY from TiN (two different thicknesses) deposited on bulk polished Nb substrates. The films were deposited and measured without atmospheric exposure.

ACKNOWLEDGEMENTS

Many colleagues have contributed to SLAC's SEY measurement program since 1975, particularly Ed Garwin who began the program and maintains a keen interest in its development. Their affiliations at the time of their contributions are listed: Ed Garwin, Frank King, Earl Hoyt, Frederic Le Pimpec, Mauro Pivi, and Ali-Reza Nyaiesh, SLAC; Takashi Momose, Tohoku University; Osamu Aita, Osaka Prefecture University; Erhard Kisker, KFA, Julich; and Pilar Prieto, Universidad Autónoma Madrid.

REFERENCES

[1] H. Seiler, J. Appl. Phys. **54** (1983) R1.
[2] R. E. Kirby, E. L. Garwin, F. K. King and A. R. Nyaiesh, J. Appl. Phys. **62** (1987) 1400.
[3] E. L. Garwin, F. K. King, R. E. Kirby and O. Aita, J. Appl. Phys. **61** (1987) 1145.
[4] E. L. Garwin, E. W. Hoyt, R. E. Kirby and T. Momose, J. Appl. Phys **59** (1986) 3245.
[5] R. E. Kirby and F. K. King., Nucl. Instr. and Meth. in Phys. Research A**469** (2001) 1.
[6] Varian, Inc. integral Auger electron gun, model 2611.
[7] POCO Graphite, Inc., type AXF-5Q.
[8] J. A. Cross, J. Phys. D**6** (1973) 622.
[9] M. Q. Ding and E. M. Williams, Vacuum **39** (1989) 463.
[10] J. Halbritter, J. de Physique **45** (1984) C2.
[11] I. Popova, V. Zhukov and J. T. Yates, Jr., Appl. Physics Lett. **75** (1999) 3108.
[12] R. Patel, Q. Guo, I. Cocks, E. M. Williams, E. Roman and J. L. de Segovia, J. Vac. Sci. Technol. A**15** (1997) 2553.
[13] W. Gopel, J. A. Anderson, D. Frankel, M. Jaehnig, K. Phillips, J. A. Schafer and G. Rocker, Surf. Science **139** (1984) 333.
[14] E. L. Garwin, E. W. Hoyt, M. Rabinowitz and J. Jurow, Proc. Fourth Int. Vacuum Congr., Manchester Pt. **1** (1968) 131.